ELSEVIER

Ceramics International 32 (2006) 819–824

CERAMICS INTERNATIONAL

www.elsevier.com/locate/ceramint

Preparation of mesoporous titania nanocrystals using alkylamine surfactant templates

Naoki Koshitani, Singto Sakulkhaemaruethai [1], Yoshikazu Suzuki, Susumu Yoshikawa *

Institute of Advanced Energy, Kyoto University, Gokasho, Uji, Kyoto 611-0011 Japan

Received 30 March 2005; received in revised form 12 May 2005; accepted 6 June 2005
Available online 19 August 2005

Abstract

Mesoporous titania nanocrystals were obtained through the surfactant-assisted templating method (SATM). The synthesis was carried out in the presence of two series of micellar surfactant systems, namely $(C_nH_{2n+1})_2NCH_3$ and $(C_nH_{2n+1})NH_2$ with $n = 8$–14. The sol–gel processed nanocrystalline titania were characterized by small angle X-ray scattering (SAXS), transmission electron microscopy (TEM), X-ray diffraction (XRD), N_2 adsorption–desorption measurements. The morphologies of titania were affected by the formation conditions, e.g., carbon chain length of hydrophilic tails of alkylamine surfactants, and calcination conditions. SAXS experiments indicated that the structure of titania sol under SATM was explained by the mass fractal model. The synthesized powders exhibited anatase-type mesoporous structure with surface area of up to 215 $m^2\ g^{-1}$.

Keywords: A. Calcination; A. Sol–gel processes; D. TiO_2; Surfactant-assisted templating method

1. Introduction

Titania (TiO_2) nanomaterials have attracted a lot of interest from both theoretical and practical point of views as an attractive material for oxide semiconductors. Considerable efforts have been devoted to develop titania nanomaterials with well-structured, porous, high surface area, and high photocatalytic activity [1–3], stimulated by the successful synthesis of the mesoporous molecular sieves family, M41S [4,5].

The formation approaches of titania nanomaterials using self-assemble of surfactant as templating structures have been reported by several groups [6–8]. Antonelli and Ying [6] have reported the preparation of mesoporous titania through a modified sol–gel process in presence of phosphate surfactant. Yang et al. [8] prepared mesoporous titania using poly(alkylene oxide) block copolymers as template structures and titanium inorganic salts as metal precursor in a non-aqueous solution. A number of formation mechanism models have been proposed to explain the growth process of nanostructured materials from the inorganic precursor in the presence of surfactants self-assembles [9,10]. However, the growth process and self-assembly mechanism, which drive both organic and inorganic phases to coexist in a well-defined mesostructure within the final materials, are far from being well understood. The effective alternative approach, called surfactant-assisted templating method (SATM), for fabricating titania nanocrystals with high quality has been reported [11–13]. The titania nanocrystals, obtained from this approach using tetra(*i*-propyl) orthotitanate (TIPT)–acetylacetone (ACA)–laurylamine hydrochloride (LAHC) system, exhibited anatase-type mesoporous structure with surface area of up to 140 $m^2\ g^{-1}$. The structural and morphological characteristics of synthesized titania nanocrystals were affected by various key parameters, i.e., surfactant-removing condition, surfactant to alkoxide ratio, acetylacetone concentration, etc.

In this paper, the formation and characterization of mesoporous titania nanocrystals in TIPT–ACA–alkylamine

* Corresponding author. Tel.: +81 774 38 3502; fax: +81 774 38 3508.
E-mail addresses: s_singto@hotmail.com (S. Sakulkhaemaruethai), s-yoshi@iae.kyoto-u.ac.jp (S. Yoshikawa).
[1] Present address: Chemical Research Institute, Rajamangala University of Technology, Klong 6, Thanyaburi, Pathumthani 12110, Thailand. Tel.: +66 2549 3527; fax: +66 2549 3526.

0272-8842/$30.00
doi:10.1016/j.ceramint.2005.06.009

surfactant systems under sol–gel process, in which gelation occur homogeneously, will be described. The morphology of titania under sol–gel process in the presence of micellar surfactant solution is elucidated with SAXS, TEM, XRD, N_2 adsorption–desorption measurements.

2. Experimental procedure

2.1. Titania nanocrystals preparation

Mesoporous titania nanocrystals were prepared under the controllable sol–gel process of titanium alkoxide in the presence of micellar surfactants, i.e., double-chained alkylamine surfactants, $[(C_nH_{2n+1})_2NCH_3$ ($n = 8$, 10, 12, 14)], and long chain alkylamine surfactants, $[C_nH_{2n+1}NH_2$ ($n = 8$, 10, 12, 14)] as templating structures. Tetra(*i*-propyl) orthotitanate (as a titania precursor), was modified with acetylacetone resulting the yellow TIPT–ACA adduct. The composition of TIPT to ACA was 1:1 in molar ratio. In separate beaker, surfactant and HCl were dissolved in deionized water at 40 °C until homogeneous solution is obtained. The composition molar ratio of surfactant to acid was 1:1. The mixture of TIPT–ACA was slowly added under magnetic stirring to the micellar surfactant solution at room temperature. The composition ratio of alkylamine surfactant to TIPT was 1:4. The resulting suspension was stirred for 1 h, further stirred at 40 °C for 48 h, and kept sealed under static condition at 80 °C for 1 week. The resulting titania gel with yellow mother liquor was dried at 80 °C for overnight, and washed with *i*-propanol (IPA). The powder was again dried at 80 °C in air and calcined at temperature in the range of 250–450 °C at given time.

2.2. Characterization

The nanostructure of the titania sol was studied by small angle X-ray scattering (SAXS) (Rigaku Rotaflex, RU-200) using Cu Kα radiation under operating conditions of 40 kV, 80 mA. The scattering pattern was recorded in the range of 0.1–4.0° (2θ) with step 0.05° (2θ). The background scattering was subtracted from the total experimental scattering intensity. The fractal dimension (D_f) and the radius of gyration (R_g) were determined by analysis of mass fractal (power-law) and the Guinier regions, respectively [14]. Transmission electron microscopy (TEM) and selected area electron diffraction (SAED) were performed on a transmission electron microscope (JEOL JEM-200CX) at 200 kV. Constituent phases were determined by X-ray diffractometer (Model RINT-2100, Rigaku) with Cu Kα radiation ($\lambda = 0.154$ nm) at 40 kV and 40 mA, and a scan rate of 2°(2θ)/min. N_2 adsorption–desorption isotherms were obtained with a nitrogen adsorption apparatus (BELSORP18 PLUS). The powders were further degassed under vacuum at 200 °C for 2 h before measurements to evacuate the physisorbed moisture.

3. Results and discussion

3.1. Structural evolution of titania in sol–gel process

Titania sol was prepared through SATM using TIPT–ACA–$[(C_nH_{2n+1})_2NCH_3$ ($n = 8$, 10, 12, 14)] system. After kept at 40 °C for 48 h, the homogeneous sol was characterized the fractal morphology by SAXS. Fig. 1 shows a SAXS profile of titania sol prepared using $(C_8H_{17})_2NCH_3$ as templating structures at starting reaction ($t = 0$ h) in 80 °C. As seen in this figure, fitting between $\ln(q) = -1.5$ and 0.5 gives a straight line with negative slope corresponding to a mass fractal scaling laws [15]. The negative slope was measured as −1.61 ($D_f = 1.61$), which represents the growth of rather linearly connected fractal [16]. Fitting between $\ln(q) = -1.5$ to 0.5, gives an intersection between fractal behavior to the Guinier region at $\ln(q) = -1.54$, i.e., $q = 0.214$. SAXS data in Fig. 1 was replotted as Guinier plot as given in Fig. 2. In Guinier region, where the system is diluted and monodisperse [14], Guinier's approximation: $\ln I(q) = \ln I(0) - (1/3)R_g^2 q^2$ was expressed [17]. The R_g can be estimated from slope of linear regressive line in Guinier plot (Fig. 2). The slope was measured as −17.31, then R_g was estimated as 7.21 nm.

The time evolutions (reaction occur at 80 °C) of estimated D_f and R_g of titania sol derived from different type of double-chained alkylamine surfactants $[(C_nH_{2n+1})_2NCH_3$ ($n = 8$, 10, 12, 14)] are given in Fig. 3. As seen in this figure, the increase of the aging time of titania sol at 80 °C results in an increase of both D_f and R_g. The morphologies of all titania materials derived under TIPT–ACA–$[(C_nH_{2n+1})_2NCH_3$ ($n = 8$, 10, 12, 14)] system are nanoscale mass fractals with $R_g > 12$ nm and D_f in the range of 1.9–2.1, which are grown by a diffusion-limited cluster–cluster aggregation process [16]. Similarly, SAXS analysis has been performed on titania sol derived with long chain alkylamine surfactants $[C_nH_{2n+1}NH_2$ ($n = 8, 10, 12$, 14)]. The dependence of D_f and R_g as a function of aging time (at 80 °C) of all samples are given in Fig. 4. It can be noticed that the aggregates generated in titania derived with

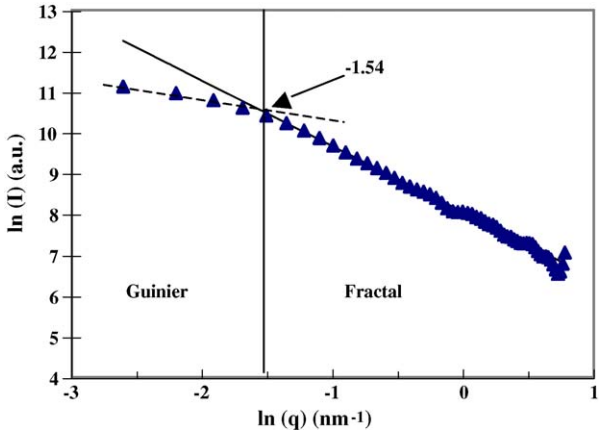

Fig. 1. SAXS profile of titania sol derived from TIPT–ACA–$(C_8H_{17})_2NCH_3$ system.

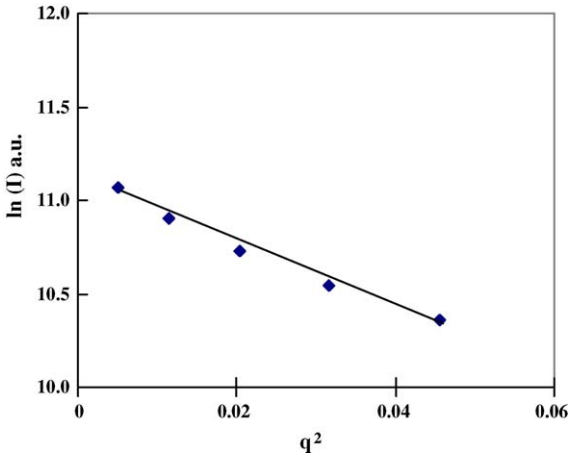

Fig. 2. Guinier plot of SAXS spectrum of titania sol derived from TIPT–ACA–$(C_8H_{17})_2NCH_3$ system.

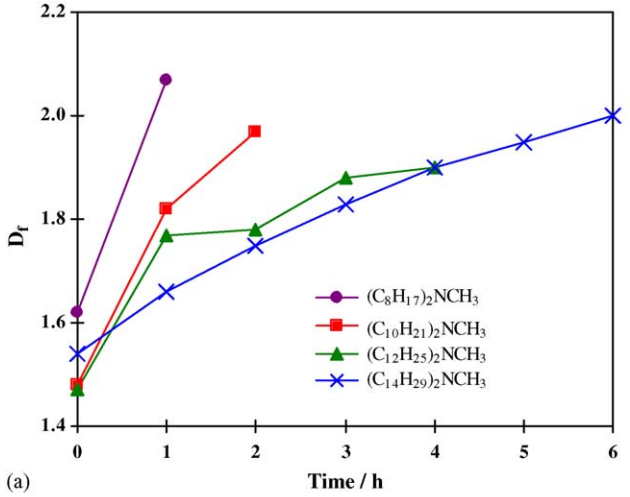

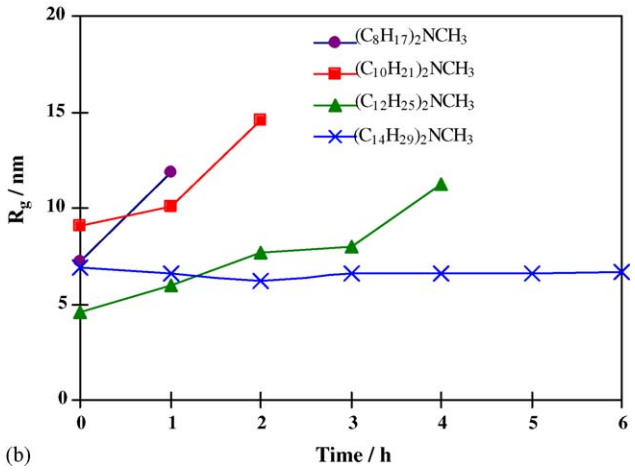

Fig. 3. Dependence of (a) D_f and (b) R_g as a function of aging time of titania sol derived in variation of double-chained alkylamine surfactants $[(C_nH_{2n+1})_2NCH_3$ (n = 8, 10, 12, 14)] aqueous solution.

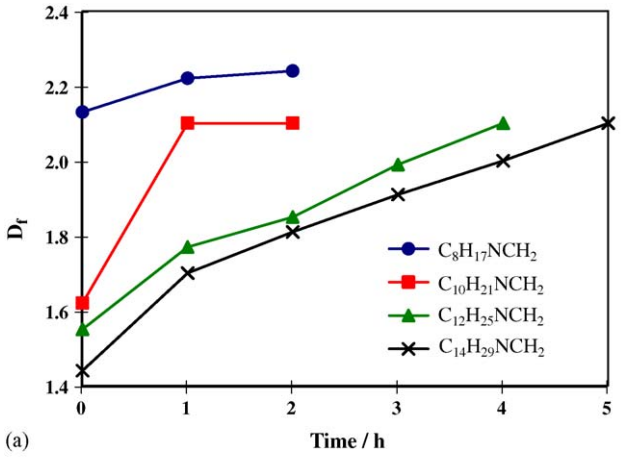

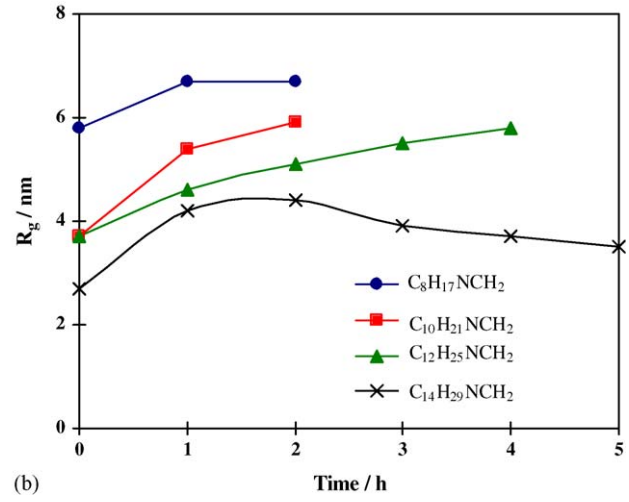

Fig. 4. Dependence of (a) D_f and (b) R_g as a function of aging time of titania sol derived in variation of alkylamine surfactants $[C_nH_{2n+1}NH_2$ (n = 8, 10, 12, 14)] aqueous solution.

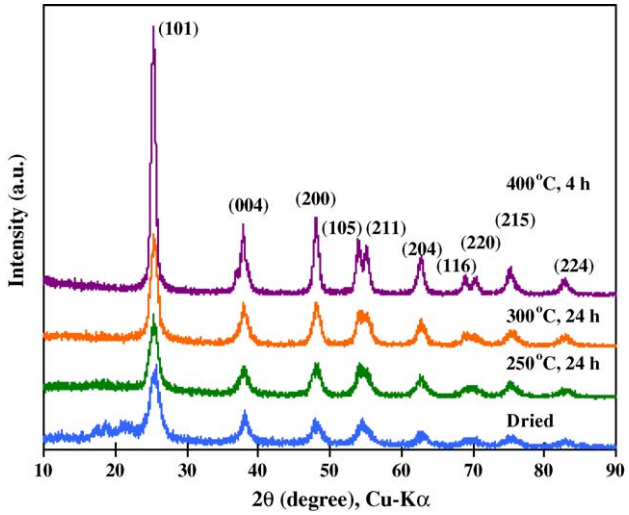

Fig. 5. XRD patterns of anatase-type titania nanocrystals prepared at different calcination conditions.

Table 1
FWHM and crystallite sizes obtained from the XRD results for titania nanocrystals calcined at different conditions in air atmosphere

Calcination condition	FWHM[a]	Crystallite size[b] (nm)
Dried powder	1.24	6.5
250 °C for 24 h	0.94	8.5
300 °C for 24 h	0.87	9.3
400 °C for 24 h	0.73	11

[a] Full-width at half maximum intensity of the (1 0 1) diffraction peak.
[b] Estimated by using Debye–Scherrer equation.

TIPT–ACA–[$C_nH_{2n+1}NH_2$ (n = 8, 10, 12, 14)] system form more compact branched fractal than that of nanocrystals derived with TIPT–ACA–$(C_nH_{2n+1})_2NCH_3$ system, with R_g in the range of 11–14 nm and D_f in the range of 2.1–2.2, which follows a diffusion-limited monomer–cluster aggregation process [16].

3.2. Morphology of titania nanocrystals

Fig. 5 shows the XRD patterns of titania nanocrystals calcined at different conditions. All sample powders are crystalline. The XRD pattern of all powders are similar and peaks are assigned to the (1 0 1), (0 0 4), (2 0 0), (1 0 5) reflections of the anatase phase. Crystallinity of the titania nanocrystals calcined at different temperatures has been studied. The full-width at half maximum intensity (FWHM) of (1 0 1) diffraction peak and the crystallite size of titania nanocrystals estimated from the Debye–Scherrer's equation [18] using the XRD line broadening were reported in Table 1. As seen in Fig. 5 and Table 1, the crystallinity of nanocrystals increased (XRD became sharper, and FWHM decreased) as the calcination temperatures increased. At higher calcination temperatures, the crystallite sizes formed are larger in size, which can be attributed to the thermally promoted crystallite growth. These results were in agreement with the previous reported by Yu et al. [19]. Fig. 6 shows high resolution TEM image and SAED pattern of mesoporous titania nanocrystals calcined at 500 °C for 4 h. As seen in this figure, the bulk calcined titania powder consisted of ~10 nm particles. The first four rings of SAED, shown in inset of Fig. 6, are assigned to the reflections of the anatase phase. The results are in agreement with the XRD results shown in Fig. 5. Examples of the N_2 adsorption–desorption isotherms and pore size distributions of mesoporous titania nanocrystals derived with this proposed approach are shown in Fig. 7. The isotherms exhibit the typical type IV, characteristic of mesoporous materials according to the IUPAC classification [20]. The dependence of Brunauer–Emmett–Teller surface area (S_{BET}) and pore diameter of synthesized titania nanocrystals derived with different carbon chain length of hydrophobic tails of surfactants in aqueous solution are displayed in

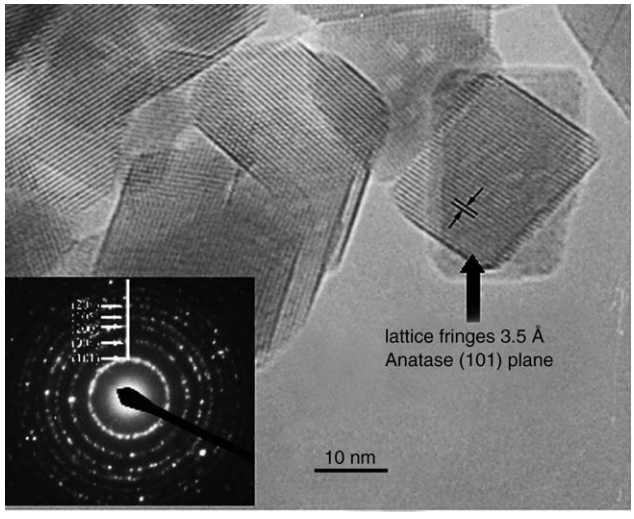

Fig. 6. High-resolution TEM image and SAED pattern of titania nanocrystals calcined at 500 °C for 4 h.

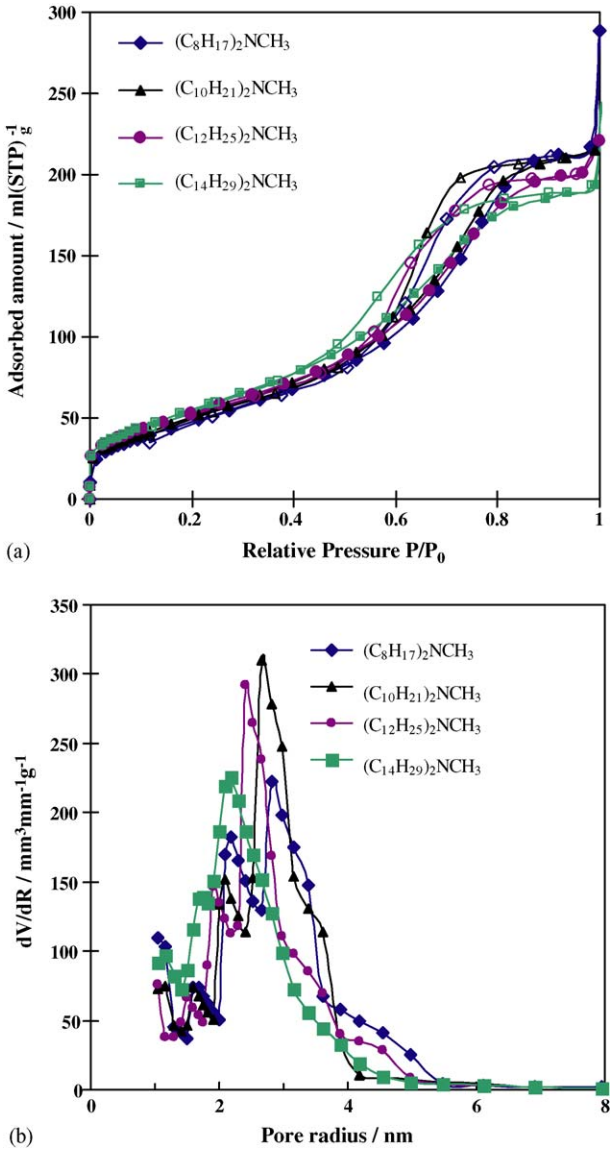

Fig. 7. (a) N_2 adsorption–desorption isotherms and (b) pore size distribution curves of titania nanocrystals derived with TIPT–ACA–$(C_nH_{2n+1})_2NCH_3$ (n = 8, 10, 12, 14) system.

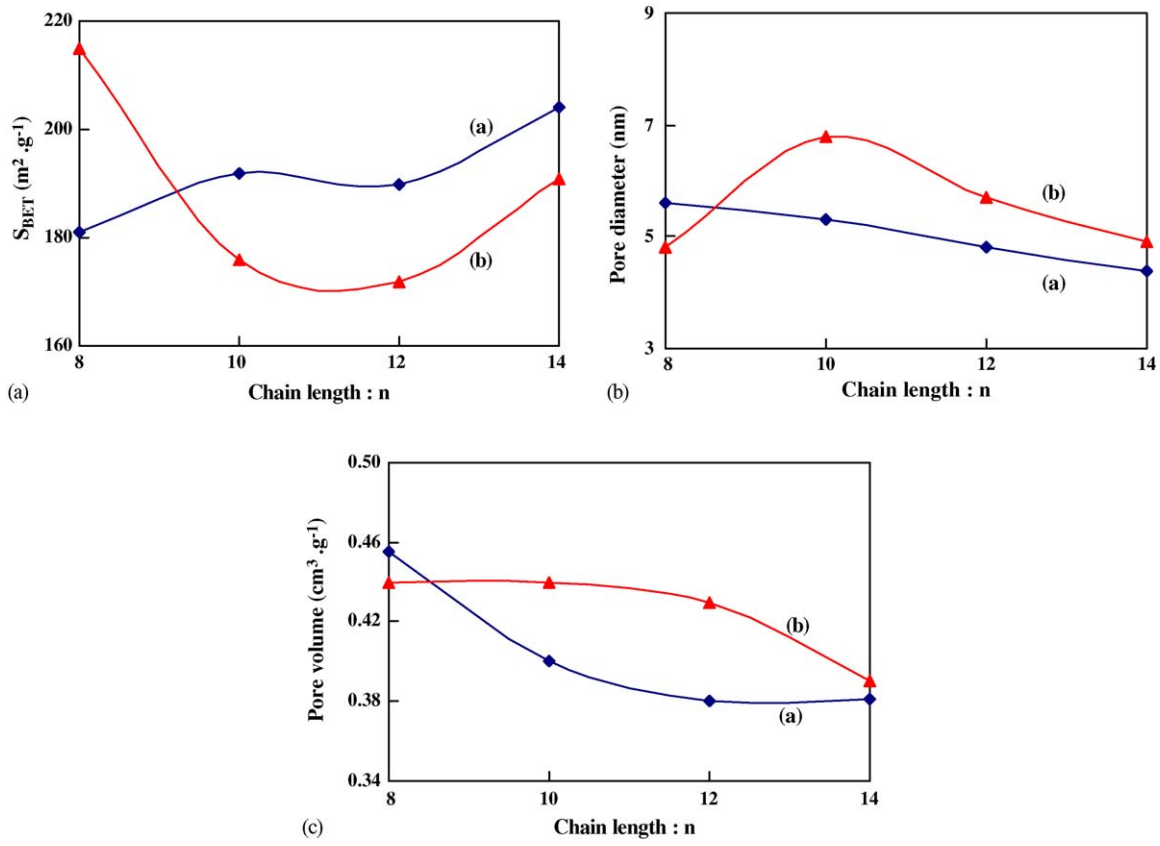

Fig. 8. Dependence of S_{BET}, pore diameter, and pore volume of titania nanocrystals on the carbon chain length of hydrophobic tail of (a) $(C_nH_{2n+1})_2NCH_3$ and (b) $C_nH_{2n+1}NH_2$ (n = 8, 10, 12, 14).

Fig. 8. The calcined titania nanocrystals derived with $(C_nH_{2n+1})_2NCH_3$ (n = 8, 10, 12, 14), as templating structures exhibit S_{BET} in the range of 180–200 $m^2\ g^{-1}$, pore diameter in the range of 4.5–6 nm, and pore volume in the range of 0.38–0.46 ml g^{-1}. The calcined titania nanocrystals derived with $C_nH_{2n+1}NH_2$ (n = 8, 10, 12, 14), as templating structures exhibit S_{BET} in the range of 170–215 $m^2\ g^{-1}$, pore diameter in the range of 5–7 nm, and pore volume in the range of 0.38–0.44 ml g^{-1}.

3.3. Possible formation mechanism of titania nanocrystals

The formation mechanism of titania nanocrystals through SATM approach is still unclear at this point. However, it is agreed based on the formation of silica molecular sieves using surfactants as templating structures that the formation process of titania nanocrystals in this system through the geometric matching between titania species (I^+), surfactant head group (S^+), and counter ions (X^-) in an acidic aqueous solution system and the controllable sol–gel process [21]. ACA played a role as a modifying agent to retard hydrolysis reaction of titanium alkoxide by coordinate to the central metal atom of titania precursor and letting one isopropoxyl group unbound [22]. When the chemical modified titania precursor and alkylamine micellar acidic solution was mixed, the partially hydrolyzed precursor was formed and interacted with head group of surfactant. Further gelation process followed the formation of –O–Ti–O–Ti– network by polycondensation on the surface of assemblies resulting in the production of mesoporous structure.

4. Conclusion

Mesoporous titania nanocrystals have been synthesized through SATM under sol–gel process in the presence of alkylamine surfactant as templating structures. The synthesized titania aggregates are nanoscale mass fractals. The fractal dimensions displays in the range from 1.9 to 2.1 and form 2.1 to 2.2 for titania sol derived using $[(C_nH_{2n+1})_2NCH_3]$ and $[C_nH_{2n+1}NH_2]$ (n = 8–14), respectively. The surface area of calcined titania nanocrystals prepared through this proposed approach can exceed 215 $m^2\ g^{-1}$ and decrease as the calcination temperature increases. The surfactant system played an important role on the structural and morphological characteristics of titania.

Acknowledgements

This work was supported by a grant-in-aid from the Ministry of Education, Science, Sports, and Culture of Japan

under the 21COE program ''Establishment of COE on Sustainable Energy System'', and ''Nanotechnology Support Project''. The authors wish to thank Professor Seiji Isoda, Professor Hiroki Kurata of the Institute for Chemical Research, Kyoto University, for the use of TEM apparatus, and Professor Toshinobu Yoko of the Institute for Chemical Research, Kyoto University, for the use of XRD equipment.

References

[1] D.M. Antonelli, Synthesis of phosphorus-free mesoporous titania via templating with amine surfactants, Microporous Mesoporous Mater. 30 (1999) 315–319.
[2] H. Yoshitake, T. Sugihara, T. Tatsumi, Preparation of wormhole-like mesoporous TiO_2 with an extremely large surface area and stabilization of its surface by chemical vapor deposition, Chem. Mater. 14 (2002) 1023–1029.
[3] T. Peng, A. Hasegawa, J. Qiu, K. Hirao, Fabrication of titania tubules with high surface area and well-developed mesostructural walls by surfactant-mediated templating method, Chem. Mater. 15 (2003) 2011–2016.
[4] C.T. Kresge, M.E. Leonowicz, W.J. Roth, J.C. Vartuli, J.S. Beck, Ordered mesoporous molecular sieves synthesized by a liquid-crystal template mechanism, Nature 359 (1992) 710–712.
[5] J.S. Beck, J.C. Vartuli, W.J. Roth, M.E. Leonowicz, C.T. Kresge, K.D. Schmitt, T.T.-W. Chu, D.H. Olson, E.W. Sheppard, S.B. McCullen, J.B. Higgins, J.L. Schlenker, A new family of mesoporous molecular sieves prepared with liquid crystal templates, J. Am. Chem. Soc. 114 (1992) 10834–10843.
[6] D.M. Antonelli, J.Y. Ying, Synthesis of hexagonally packed mesoporous TiO_2 by a modified sol–gel method, Angew. Chem. Int. Ed. Engl. 34 (1995) 2014–2017.
[7] H. Hirashima, H. Imai, V. Balek, Preparation of meso-porous TiO_2 gels and their characterization, J. Non-Cryst. Solids 285 (2001) 96–100.
[8] P. Yang, D. Zhao, D.I. Margolese, B.F. Chmelka, G.D. Stucky, Block copolymer templating syntheses of mesoporous metal oxides with large ordering lengths and semicrystalline framework, Chem. Mater. 11 (1999) 2813–2826.
[9] S. Peres-Durand, J. Rouviere, C. Guizard, Sol–gel processing of titania using reverse micellar systems as reaction media, Colloids Surf. A: Physicochem. Eng. Aspects 98 (1995) 251–270.
[10] H. Naono, M. Hakuman, T. Tsunehira, N. Tamura, K. Nakai, Formation process of MCM-41 precursor and porous texture of MCM-41, J. Colloid Interface Sci. 224 (2000) 358–365.
[11] M. Adachi, Y. Murata, H. Harada, S. Yoshikawa, Formation of titania nanotubes with high photo-catalytic activity, Chem. Lett. (2000) 942–943.
[12] S. Sakulkhaemaruethai, Y. Suzuki, S. Yoshikawa, Surfactant-assisted preparation and characterization of mesoporous titania nanocrystals—effect of various processing conditions, J. Ceram. Soc. Jpn. 112 (10) (2004) 547–552.
[13] S. Sakulkhaemaruethai, Y. Suzuki, S. Yoshikawa, Effect of ZrO_2-addition on structure of sol–gel derived TiO_2 nanopowder, J. Jpn. Soc. Powd. Powd. Metal 51 (11) (2004) 789–794.
[14] J. Teixara, in: H.E. Stanley, E.N. Ostrowsky (Eds.), On Growth and Form, Martinus Nijhoff, Boston, MA, 1986, p. 145.
[15] P.W. Schmidt, Small-angle scattering studied of disordered, porous and fractal systems, J. Appl. Cryst. 24 (1991) 414–435.
[16] P. Meakin, in: H.E. Stanley, E.N. Ostrowsky (Eds.), On Growth and Form, Martinus Nijhoff, Boston, MA, 1986, pp. 111–135.
[17] A. Guinier, G. Fournet, Small-Angle Scattering of X-rays, John Wiley & Sons, New York, 1955.
[18] R. Jenkins, R.L. Snyder, Introduction to X-ray Powder Diffractometry, John Wiley & Sons, New York, 1996, 89-91.
[19] J.G. Yu, J.C. Yu, W. Ho, M.K.-P. Leung, B. Cheng, G. Zhang, X. Zhao, Effect of alcohol content and calcination temperature on the textural properties of bimodally mesoporous titania, Appl. Catal. A: Gen. 255 (2003) 309–320.
[20] K.S.W. Sing, D.H. Everett, R.A.W. Haul, L. Moscow, R.A. Pierotti, J. Rouquerol, T. Siemieniewska, Reporting physisorption data for gas/solid systems with special reference to the determination of surface area and porosity, Pure Appl. Chem. 57 (1985) 603–619.
[21] S. Schacht, Q. Huo, I.G. Voigt-Martin, G.D. Stucky, F. Schüth, Oil–water interface templating of mesoporous macroscale structures, Science 273 (1996) 768–771.
[22] A. Ponton, S. Barboux-Doeuff, C. Sanchez, Rheology of titanium oxide based gels: determination of gelation time versus temperature, Colloids Surf. A: Physicochem. Eng. Aspects 162 (1999) 177–192.